

Photophysics of charge transfer in a polyfluorene/violanthrone blend

J. Cabanillas-Gonzalez,* T. Virgili, and G. Lanzani

IFN-CNR, Dipartimento di Fisica, ULTRAS-INFM, Politecnico di Milano, Milano 20133, Italy

S. Yeates

Electronic Materials Business, Avencia Limited, P. O. Box 42, Hexagon House, Blackley, Manchester M9 8ZS, United Kingdom

M. Ariu, J. Nelson, and D. D. C. Bradley

The Blackett Laboratory, Experimental Solid State Group, Imperial College, London SW7 2BZ, United Kingdom

(Received 1 April 2004; published 28 January 2005)

We present a study of the photophysical and photovoltaic properties of blends of violanthrone in poly[9,9-bis(2-ethylhexyl)-fluorene-2,7-diyl] (PF_{2/6}). Photoluminescence quenching and photocurrent measurements show moderate efficiencies for charge generation, characteristic of such polymer/dye blends. Pump-probe measurements on blend films suggest that while ~47% of the total exciton population dissociates within 4 ps of photoexcitation, only ~32% subsequently results in the formation of dye anions. We attribute the discrepancy to the likely formation of complex species with long lifetimes, such as stabilized interface charge pairs or exciplexes. This conclusion is supported by the appearance of a long lifetime component of 2.4 ns in the dynamics of the photoinduced absorption signal associated to polarons in photoinduced absorption bands centered at 560 nm.

DOI: 10.1103/PhysRevB.71.014211

PACS number(s): 78.47.+p, 82.53.-k, 82.53.Xa, 78.55.Kz

I. INTRODUCTION

The photovoltaic effect in polymer-based blends with heterojunction donor-acceptor interfaces has been widely studied in the literature.¹⁻⁴ Among all material combinations, polymer/fullerene blends have attracted particular attention due to the large charge photogeneration efficiency that arises from the notable electron acceptor properties of fullerenes.^{1,2} Fullerene doping is, however, not equally effective in all conjugated polymers.^{2,5} It has been argued that large substitute groups can act to keep the fullerene molecules at a substantial distance from the polymer backbone and this results in limited photoinduced electron transfer.⁵ It has been further suggested that in these latter sorts of blend, photoinduced electron transfer is a complex process that involves three steps: (i) exciton dissociation, (ii) formation of stable polaron pairs at the donor-acceptor interface, and (iii) electron transfer on long time scales. In order to improve the efficiency for photoinduced electron transfer, chemical substitutions have been made to improve the cosolubility, and thus achieve larger donor-acceptor interpenetration in the blend.⁶

Dyes on the other hand have also been employed as electron acceptors blended on polymer leading to moderate photovoltaic performances, which have been understood as due to the tendency of dye molecules to form isolated domains inside the polymer matrix, preventing therefore efficient charge collection.⁷ In some polymer/dye blends it has been demonstrated that inducing dye crystallization in the polymer matrix can lead to an enhancement of photocurrent efficiency by a factor of 2 or more.^{7,8} This improvement is considered to be the result of an increase in charge-carrier mobility within the dye crystallites with respect to the amorphous dye. In addition, the large exciton diffusion lengths characteristic of organic crystals (2.5 μm is measured in perylene diimides⁹) help to ensure charge photogeneration even in

situations of large scale phase separation. In spite of these improvements, the photocurrent efficiencies of polymer/dye solar cells remain still well below the best values found from polymer/fullerene blends.^{1,2} Hence, there seem to be evidences that their poor performance could be conditioned by an inefficient photoinduced charge-transfer process besides of the limited charge mobility exhibited in blend films.

In this paper photocurrent measurements are combined with photophysical studies in order to establish a picture of the charge transfer process in poly[9,9-bis(2-ethylhexyl)-fluorene-2,7-diyl] (PF_{2/6})/violanthrone blends. Violanthrone (also named as dibenzathrone) is a dye molecule with notable photoconductivity properties which has attracted interest in the field of electrophotography for photocopiers.²⁴ We have chosen PF_{2/6} as the donor material due to the nondispersive hole transport and large mobilities exhibited by related dialkyl polyfluorenes at room temperature.¹⁰ By performing pump-probe measurements on a 10:100 violanthrone:PF_{2/6} weight ratio blend film, we have obtained both PF_{2/6} polaron and violanthrone anion populations at early times after pump excitation. Comparison between the population of these species and the total number of quenched singlets in PF_{2/6} provides us with a quantitative measurement of the charge-transfer efficiency as well as an insight into the nature of the mechanism.

II. EXPERIMENTAL METHOD

The preparation of blend films involved processing of the materials in solution and subsequent Spincoating. Dye was dispersed on polymer by blending two master chloroform solutions of pure PF_{2/6} and pure violanthrone in different amounts, keeping constant the total material concentration in each blend solution (8 mg/ml). Spin coating of blend solu-

tions on SiO₂ silica spectroil substrates at 1500 rpm produced films with a thickness of approximately 90 nm. For electrical characterization, devices were fabricated in a sandwich configuration by Spin coating the blends on top of PEDOT:PSS (Baytron PTM) coated Balzers 30 Ω/cm² indium tin oxide substrates and depositing aluminum cathodes on top of the blend films via thermal evaporation. Photoluminescence (PL) was excited with a 354 nm He-Cd laser with a power intensity typically below 1 mW/cm². The sample was placed inside an integrating sphere in N₂ atmosphere in order to avoid photo-oxidation. The PL emission was collected with an optic fibre and delivered to a Spex 270M scanning monochromator before detection with a photomultiplier. Photoluminescence quantum efficiency (PLQE) values were calculated by integrating separately the corresponding PL spectral area of each component in blend and dividing it by the difference between the laser peak areas before and after transmission through the sample. Photocurrent measurements were performed using a Bentham illuminator Xe lamp as the excitation source. The light was selected with a monochromator and collimated by a set of lenses producing a spot of 2 cm radius that provided homogeneous illumination to each device (area=4.5 mm²). Measurements were performed in vacuum at a pressure of 10⁻² mbar. The photocurrent signal at each wavelength was detected with a high-voltage source measure unit Keithley SMU 237. The experiment was controlled with a Labview program, which synchronized each step of the monochromator with a reading of current. The average time between two scans was approximately 6 s. The external quantum efficiency (EQE) values, were obtained using a UV-818 Newport calibrated photodiode. Time-resolved photoinduced absorption experiments were performed using a 390 nm excitation beam derived from the second harmonic of the 780 nm, 150 fs pulses provided by a Kerr-lens mode-locked Ti:sapphire laser with an energy per pulse of 750 μJ at 1 KHz repetition rate. The excitation beam was split into a pump beam, which was chopped at 500 Hz and focused onto the sample, and a probe beam which was delayed with respect to the pump and focused on a sapphire plate to generate a white light continuum. The latter was focused on the sample so as to overlap the same spot on which the pump was incident. Measurements were performed with the sample enclosed in a vacuum chamber at 10⁻³ mbar. Wavelength-selective detection was achieved by placing interference filters in front of a photodiode. The signal was sent to a lock-in amplifier referred to the chopping frequency and analyzed with a custom software designed for the setup.

III. RESULTS AND DISCUSSION

A. Absorption and photoluminescence spectra

The PF_{2/6} absorption and PL spectra are depicted in Fig. 1. The spectra show features that are very reminiscent of those for poly(9,9-dioctylfluorene) (PFO):¹¹ a broad absorption band with a maximum at 390 nm and PL spectrum with vibronic peaks at 424, 444, 474, and 506 nm. The absorption spectrum of violanthrone dispersed in inert matrix of poly(methyl methacrylate) (PMMA) (dashed line in Fig. 1) is

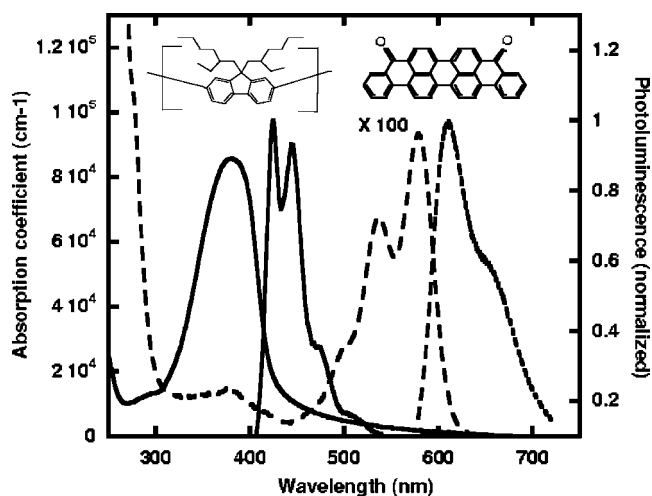


FIG. 1. Absorption and PL spectra of thin films of PF_{2/6} (bold line) and violanthrone dispersed in PMMA matrix (0.5:100 weight) (dashed line). The structures of the materials are shown above their corresponding spectra.

characterized by a vibronically structured band in the visible with peaks at 495, 535, and 579 nm. The violanthrone PL spectrum is composed of a narrow peak at 610 nm with a shoulder at around 655 nm. The dilution of violanthrone in PMMA (0.5:100 weight ratio) results in a low absolute absorption coefficient, and hence the data in Fig. 1 are plotted with a one-hundred-fold magnification for clarity.

B. PL quenching

The PL spectra for the blends with different violanthrone contents dispersed in PF_{2/6} are depicted in Fig. 2. At very low concentration, the spectra show the characteristic PL features of PF_{2/6}. As the concentration rises, quenching of the polymer PL occurs. In addition, a weak band attributed to violanthrone emission is observed to grow until the 1:100 concentration is reached. Beyond this concentration, both the PF_{2/6} and violanthrone emission are quenched. The weak dye emission at moderate concentrations may originate from direct excitation of violanthrone at 354 nm, or possibly from energy transfer between PF_{2/6} and violanthrone. The general expression for the probability of energy transfer in a donor-acceptor system based on a point dipole approximation is given by:¹²

$$K_{ET} = K_0 \left(\frac{R_0}{R} \right)^6, \quad (1)$$

where K_{ET} is the rate for energy transfer, K_0 the radiative decay rate, R_0 the Förster radius which represents the strength of the energy transfer, and R is the average donor-acceptor separation. The Förster radius can be estimated from the relative overlap between the fluorescence spectrum of the donor and absorption spectrum of the acceptor using the following expressions:

$$R_0 = \left(\frac{0.5291 K^2}{N_A n^4} T \right)^{1/6}, \quad (2)$$

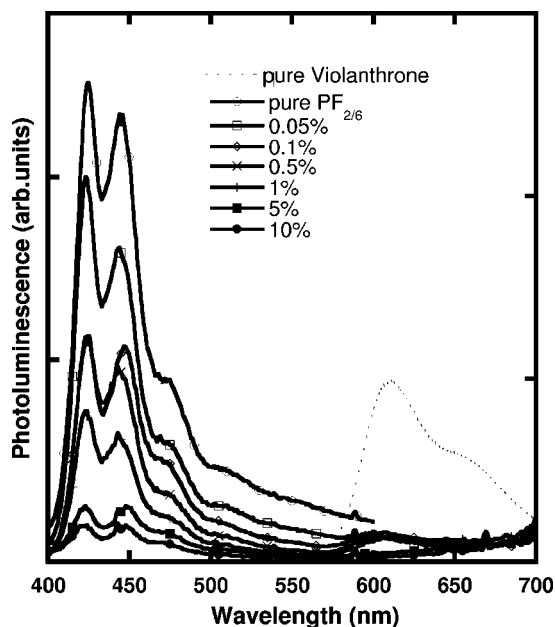


FIG. 2. PL spectra for blends of violanthrone and PF_{2/6} with different weight ratios. Excitation was with a 354 nm He-Cd laser line. The PL spectra of a 1 μm film of violanthrone dispersed in PMMA with a weight ratio 0.5:100 excited at 531 nm (dotted line) and PF_{2/6} (open circles) are also shown for comparison. The spectra were normalized to the fraction of the light absorbed by each sample. The enhancement over 650 nm is an artefact induced by the 708 nm component of the laser line.

$$T = \int_0^\infty F_m(\bar{\nu}) \epsilon_Q(\nu) \frac{d\nu}{\bar{\nu}^4}, \quad (3)$$

where K^2 is a factor that accounts for the relative orientation of donor and acceptor dipoles (2/3 for random orientation), N_A is Avogadro's number, n the refractive index of the host, and T the overlap integral [Eq. (4)] between the normalized fluorescence spectrum of the donor, F_m , and the molar decadic extinction coefficient of the acceptor ϵ_Q . In our

PF_{2/6}/violanthrone system we calculate a Förster radius of 3.3 nm, which suggests a relatively moderate energy transfer efficiency. In a 10:100 blend, for instance, where the average donor-acceptor separation is estimated to be 4.3 nm from hard-sphere considerations of the dye distribution, the decay rate ratio (K_{ET}/K_0) corresponds to 0.2, which accounts for 17% of the total photogenerated excitons undergoing energy transfer. Comparing the PL properties of violanthrone blended in an inert PMMA matrix and in PF_{2/6}, it is also possible to estimate the energy-transfer efficiency experimentally. The PLQE value for violanthrone dispersed in PMMA when the dye is directly excited at 531 nm is found to be 71%. Taking this value as the absolute PLQE of violanthrone, and the PLQE of violanthrone in a 0.5:100 blend upon exclusive polymer excitation (6%), we conclude that whether violanthrone emission is originated via energy transfer from PF_{2/6}, it would only account for 9% of the photogenerated excitons. This low energy-transfer efficiency contrasts with the 60% decrease of PF_{2/6} PLQE in the blend with respect to the pure polymer, and strongly suggests that a different mechanism is the cause of polymer PL quenching.

According to Fig. 3, the decrease in PLQE with doping is accompanied by an increase in short circuit photocurrent. Under these circumstances the electric field across the device is given by the internal field, and exciton dissociation takes place preferentially at polymer-dye interfaces if these provide a barrier for hole or electron large enough to prevent injection into the other material. At PF_{2/6}/violanthrone interfaces, electron injection from PF_{2/6} to violanthrone is favored by the 1.4 eV discontinuity of the lowest occupied molecular-orbital (LUMO) levels (Fig. 4), whereas hole injection is opposed by a 0.3 eV barrier. The increase in photocurrent with doping is normally understood as the addition of interfaces where exciton splitting can be effective. In poly(3-hexylthiophene) (P3HT)/perylene blends it has been shown, however, that low doping concentrations lead to a decrease in photocurrent efficiency due to effective trapping of electrons transferred to the dye.⁷ In our case the increase of photocurrent with doping in the low-concentration regime suggests an inefficient trapping of electrons in violanthrone domains.

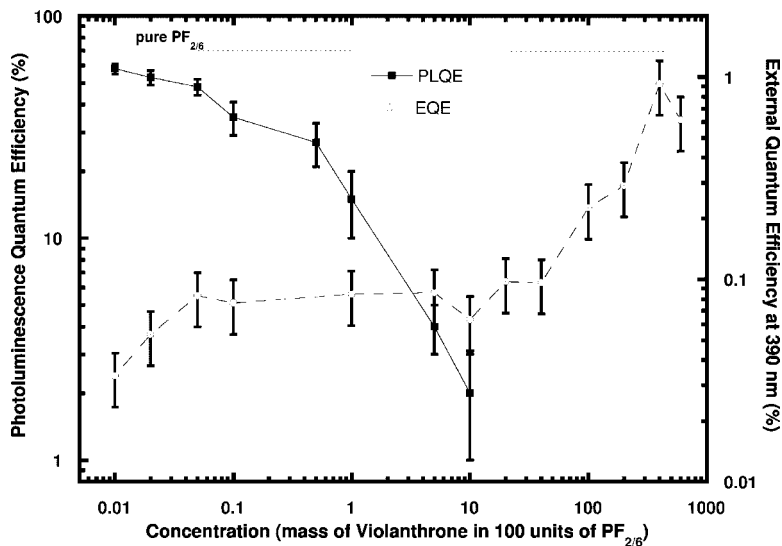


FIG. 3. A log-log plot of the dependence of PLQE (filled squares) and EQE at 0 V on the violanthrone concentration. The experimental error in the PLQE measurements was estimated as 10% of the absolute PLQE value. The error bars for the EQE data were estimated from the deviations in photocurrent values measured on six different devices.

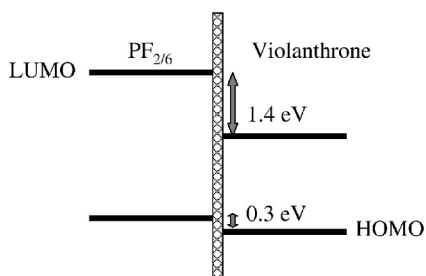


FIG. 4. Schematic of a PF_{2/6}/violanthrone heterojunction interface. The energy level offsets were deduced from cyclic voltammetry measurements reported elsewhere (Ref. 13).

The PLQE of a 10:100 blend is observed to decrease from the 64% measured in the pure PF_{2/6} polymer to only 2%, and correspondingly, the photocurrent increases by nearly one order of magnitude with respect to pure PF_{2/6}. The PL quenching factor of 32 is comparable to that found in other polymer/dye blends, (a factor of 35 was found in P3HT/perylene⁷) and some polymer/fullerene blends (a PL quenching factor of 20 was reported in ladder-type poly(paraphenylene)/fullerene¹⁴) at similar doping concentrations.

C. Photocurrent generation in blends

The EQE spectrum of the blend closely resembles the absorption spectrum, and no evidence was found for an antibatic response under the internal field condition $V_{\text{applied}}=0$ (Fig. 5). The maximum monochromatic EQE, namely 0.5%, is found at 390 nm. Upon thermal annealing, an improvement in efficiency from 0.5% to nearly 3% is achieved. In contrast to reports for some polymer/polymer blends,⁴ annealing appears to be a very effective way to improve the efficiency in polymer/dye solar cells.⁷ The reason for this enhancement is that annealing leads to the formation of dye crystalline networks embedded in the polymer bulk with two specific properties: (i) a high degree of interconnection between crystallites,¹⁵ a property that is highly desirable for a

high photocarrier collection efficiency, and (ii) submicron crystallite dimensions, which provide a large surface area and consequently many interfaces for excitons to dissociate at while traveling along the polymer chains.^{15,16} An atomic force microscopy scan of a $0.5 \mu\text{m} \times 0.5 \mu\text{m}$ area on the surface of an annealed film is shown in the inset to Fig. 5. The surface of the annealed film is characterized by needle-shaped dye crystallite structures with random orientation being the largest needles around 250 nm long. In addition, the dark areas suggest the presence of domains rich in polymer. We remark that the sixfold photocurrent improvement upon annealing significantly exceeds the twofold improvement reported for P3HT/perylene blends.⁷ Moreover, the annealing improvement in PF_{2/6}/violanthrone blends has been demonstrated to be independent of the presence of oxygen during the annealing procedure. We have not found significant differences in photocurrent generation between devices annealed in air or under N₂ atmosphere. This is a beneficial situation in respect of the development of simple processing protocols for device fabrication.

D. Photophysics of charge transfer

The steady-state spectroscopy discussed so far concerns the effect of blending with an electron acceptor dye on the PF_{2/6} singlet states. The observed decrease in singlet population is assigned to dissociation of these species at polymer / dye interfaces. A better insight into the efficiency of the electron transfer process and an understanding of the limiting factors requires one to time resolve both the formation of violanthrone anions and the increase in the PF_{2/6} polaron population that results from exciton dissociation. As can be seen in Fig. 6, the formation of violanthrone anions in chloroform solution is detected by the appearance of a new absorption band with its maximum centred around 720 nm and a shoulder at 660 nm. The strength of this absorption can be used to estimate the absorption cross section, σ using the following expressions:

$$I = I_0 e^{-\alpha d}, \tag{4}$$

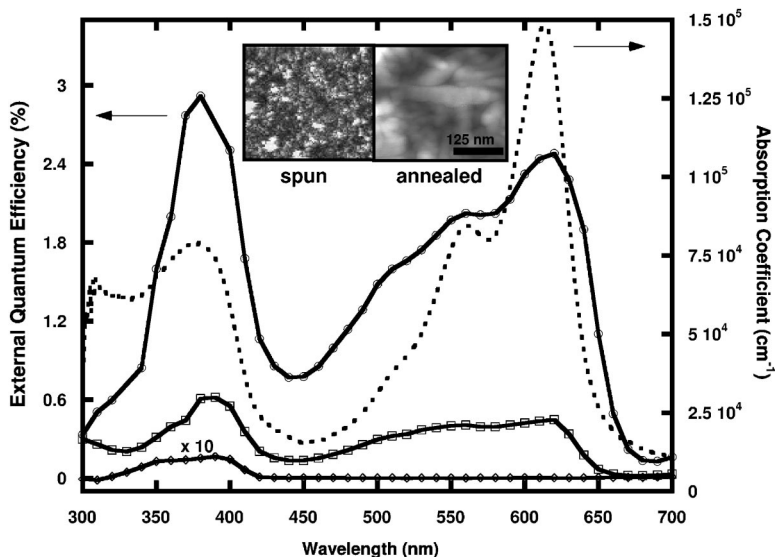


FIG. 5. The EQE spectra of devices containing PF_{2/6} (open diamonds), 6:1 violanthrone in PF_{2/6} (open squares), and the same composition subsequently annealed at 200°C in air for 5 min (open circles). The spectrum corresponding to PF_{2/6} was magnified tenfold for ease of comparison. The absorption spectrum of the 6:1 blend film (dotted line) is also shown. Inset figures show from left to right the morphologies corresponding to spun and annealed films, respectively.

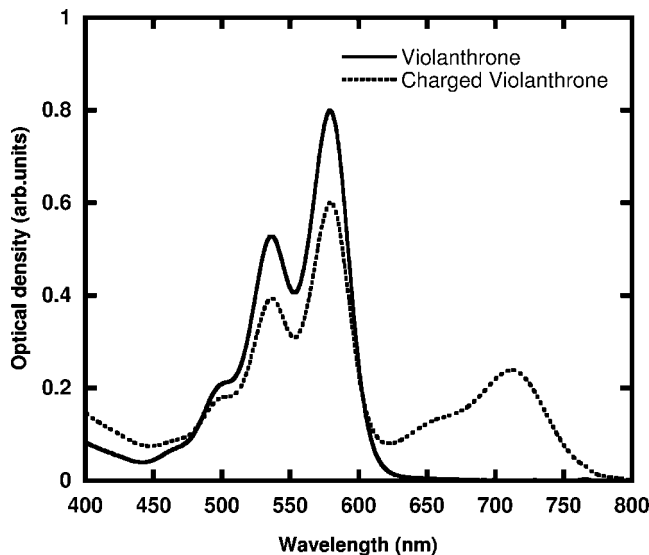


FIG. 6. Absorption spectra of violanthrone before (solid line) and after (dashed line) oxidation in solution. Oxidation was achieved by adding FeCl_3 to the solution. The additional long-wavelength (620–780 nm) band is assigned to violanthrone anion species.

$$\alpha(\lambda) = \sigma(\lambda)N, \quad (5)$$

where I and I_o are the incident and transmitted intensities, respectively, α is the absorption coefficient, d is the path length for the cuvette that contains the solution (1 cm), and N is the population density of absorbing species. A density of anions in solution, $N = 2 \times 10^{16} \text{ cm}^{-3}$, is estimated from the concentration of FeCl_3 oxidant in solution (0.03 g/l). Substituting this value in Eq. (5) together with the measured absorption coefficient gives a value for the anion absorption cross section at 720 nm, $\sigma_a^{720 \text{ nm}} = 2 \times 10^{-17} \text{ cm}^2$. This value lies reasonably below the maximum absorption cross sections reported in other dyes ($\sim 10^{-16} \text{ cm}^2$ reported for Rhodamine 640 monomers²³).

Differential transmission spectra for a film of violanthrone dispersed in PMMA (0.5:100) are displayed in Fig. 7(a). The spectra consist of a strong photobleaching (PB) signal in the region between 500 and 650 nm and a weak negative signal at wavelengths beyond 650 nm. Comparison between the absorption and PB spectra reflects a somewhat more broadened shape of the latter. A possible explanation for this effect is that the PB spectrum is influenced not only by the statistical cross-section distribution for ground state S_0 - S_n transitions, as is the case of the absorption spectrum, but also by the distribution of lifetimes for ground-state relaxation S_n - S_0 . The differential transmission spectra of $\text{PF}_{2/6}$ displayed in Fig. 7(b) shows very similar features to those previously reported in PFO:¹⁷ a region of SE below 520 nm and two photoinduced absorption (PA) bands, centered at 560 nm (PA_1) and at 760 nm (PA_2). The PA_1 band has been assigned in previous works to D_0 - D_1 transitions arising from weakly bound polaron pairs.¹⁸ These species may be created by the ultrafast exciton dissociation of singlets that are promoted into higher-lying S_n levels via two-step excitation.^{19–21} The

PA_2 band on the other hand is assigned to excited-state singlet absorption (S_1 - S_n).²¹ In a 10:100 blend, the shape of the differential transmission spectrum at 1 ps resembles that of $\text{PF}_{2/6}$. A weak broadening of the PA_2 band is, however, detected at 4 ps (Fig. 8). This broadening could arise from the overlap of the PA_2 band of $\text{PF}_{2/6}$ with the spectral region of negative signal in violanthrone that has been assigned to violanthrone anions. This observation may point towards an electron transfer to the dye taking place in the first 4 ps. We should remark that the influence of violanthrone ground state bleaching on the spectral features can be neglected due to the low absorption coefficient of violanthrone in a 10:100 blend, (inset in Fig. 8).

In order to provide a more quantitative photophysical picture we proceed to calculate the population of violanthrone anions generated by electron transfer as well as the polaron population in $\text{PF}_{2/6}$ both at 4 ps. Generically, the population density of i species [$N_i(t)$] is related to the differential transmission signal $\Delta T/T(\lambda, t)$ through the expression below:

$$\frac{\Delta T}{T}(\lambda, t) \approx \sum_{ij} N_i(t) \sigma_{ij}(\lambda) d, \quad (6)$$

where $\sigma_{ij}(\lambda)$ is the cross section for the transitions $i \rightarrow j$ and d is the thickness of the sample. Calculation of the anion population requires to evaluate the differential transmission signal at 720 nm given by the superposition between $\text{PF}_{2/6}$ excited-state singlet absorption (noted as s) and violanthrone anion absorption a :

$$\left(\frac{\Delta T}{T} \right)^{720 \text{ nm}} = \left(\frac{\Delta T}{T} \right)_s + \left(\frac{\Delta T}{T} \right)_a = (N(t)_s \sigma_s^{720 \text{ nm}} + N(t)_a \sigma_a^{720 \text{ nm}}) d. \quad (7)$$

In order to calculate the population of anions at 4 ps, $N_a(t = 4 \text{ ps})$, we must obtain first the values for the singlet population in the blend, $N_s(t = 4 \text{ ps})$, and $\sigma_s^{720 \text{ nm}}$. A value of $N_s(t = 4 \text{ ps}) = 3.7 \times 10^{19} \text{ cm}^{-3}$ was achieved by substituting in Eq. (6) the differential transmission value at 480 nm $\Delta T/T(480, 4 \text{ ps}) = 0.006$, which has only singlet contribution, and the 480 nm excited-state cross section in a pure $\text{PF}_{2/6}$ film which we estimated from the spectra in Fig. 7(b) to be $1.8 \times 10^{-17} \text{ cm}^2$. The other required parameter $\sigma_s^{720 \text{ nm}}$, can be directly addressed by substituting in Eq. (6) the differential transmission value at 720 nm in pure $\text{PF}_{2/6}$, $\Delta T/T(720, 0 \text{ ps}) = 0.01$, and the initial singlet population $9 \times 10^{19} \text{ cm}^{-3}$, producing a value of $\sigma_s^{720 \text{ nm}} = 3 \times 10^{-17} \text{ cm}^2$. Substitution of $N_s(t = 4 \text{ ps})$, $\sigma_s^{720 \text{ nm}}$, $\sigma_a^{720 \text{ nm}}$ and the differential transmission value at 720 nm $\Delta T/T(720, 4 \text{ ps}) = 0.015$ in Eq. (7) provides us with an anion population at 4 ps, of

$$N_a(t = 4 \text{ ps}) = 2.8 \times 10^{19} \text{ cm}^{-3} \pm 9.7 \times 10^{18},$$

where the uncertainty arises from the 5% relative error associated to the differential transmission values. If we consider that the total number of quenched singlets is given by

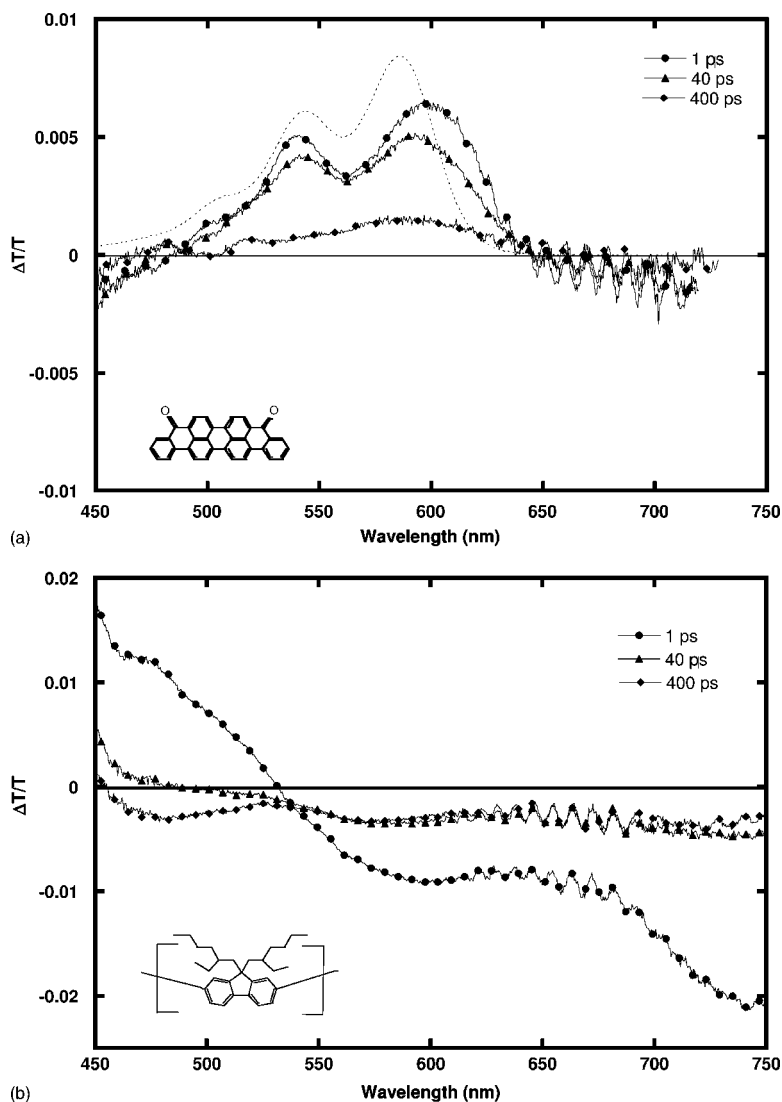


FIG. 7. (a) Differential transmission spectra recorded for a spin-coated 0.5:100 violanthrone in PMMA film at 1 ps delay (filled circles), 40 ps (filled triangles), and 400 ps (filled diamonds). The absorption spectrum of the film is also shown, offset for clarity (dotted line). (b) Differential transmission spectra of a spin-coated PF_{2/6} film at the same time delays: 1 ps (filled circles), 40 ps (filled triangles), 400 ps (filled diamonds).

$$N_{quench} = N(t=0) * (1 - \phi_{10:100}) = 8.8 \times 10^{19} \text{ cm}^{-3} \pm 4.4 \times 10^{18},$$

where $\phi_{10:100}=0.02$ is the PLQE value of PF_{2/6} in a 10:100 blend (Fig. 3), it is found that electron transfer at 4 ps appears to account for only $32\% \pm 12$ of all excitons that undergo dissociation. Concerning PF_{2/6} polaron population in the blend, a comparison with the dynamics of the pure polymer shows parallel trends during the first 3 ps followed by a slow down of the dynamics in the blend (Fig. 9). The reason for this difference is ascribed to a rise in polaron population taking place over the first ~ 7 ps, followed by a slow decay with a lifetime of approximately 2.4 ns (see inset). We remark that in a 10:100 blend, dissociation accounts for 98% of the excitons photogenerated (cf. PLQE measurements). Since a large number of these excitons are expected to be generated away from the heterojunction interfaces, the strong quenching may only be possible if it is mediated via exciton diffusion along the polymer chains. It is then expected that exciton migration will be responsible for the *dissociation lifetime*, in agreement with what has been reported in other systems.¹⁶ From the population rise experienced by polarons,

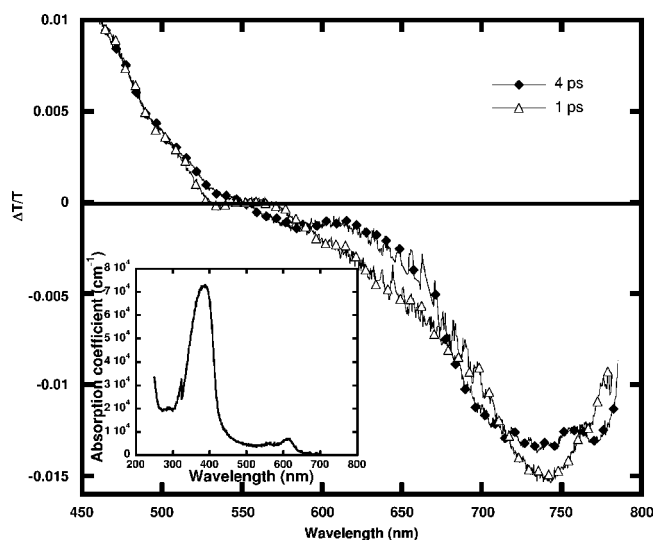


FIG. 8. Differential transmission spectra of a 10:100 violanthrone: PF_{2/6} blend at 1 ps, (dotted line, filled triangles), and 4 ps delay (bold line, filled diamonds). The lower inset shows the absorption spectrum of the film.

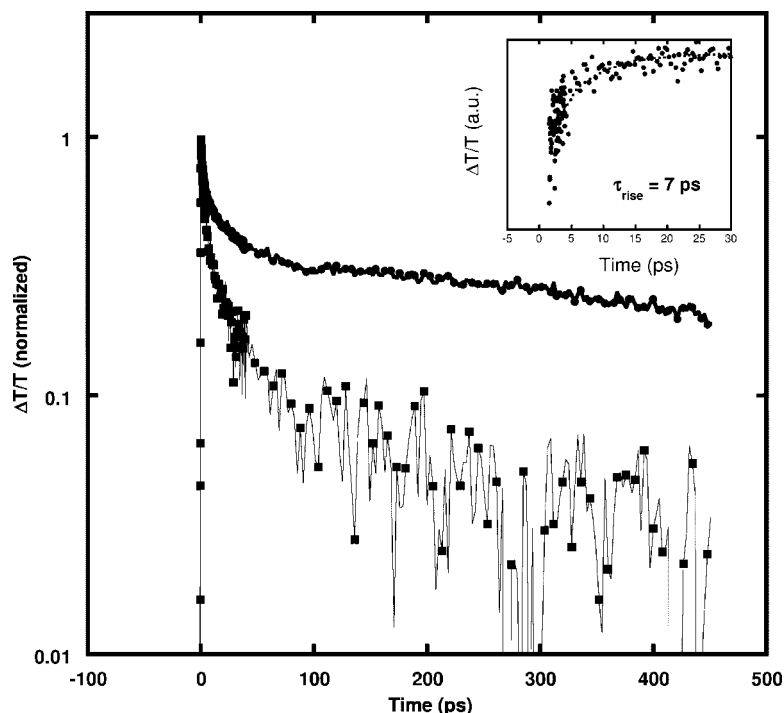


FIG. 9. Differential transmission dynamics at 560 nm for a 10:100 violanthrone: PF_{2/6} blend film (filled circles) and for PF_{2/6} (filled squares). Comparison between these data suggests a longer-lived decay in the blend. The upper inset shows the short-time rise of polaron population in the blend. This was obtained by subtracting the contribution associated to singlet and polaron-pair decay to the 560 nm blend dynamics.

we estimate that at 4 ps $47\% \pm 3$ of the excitons have already dissociated. Therefore we find a clear disagreement between the amount of excitons dissociated at 4 ps ($47\% \pm 3$) and the amount of excitons undergoing photoinduced electron transfer ($32\% \pm 12$). These discrepancies between the populations of PF_{2/6} polarons and violanthrone anions could be the result of a complex electron transfer process involving the formation of intermediate species. In some polymer blends it has been reported that exciton dissociation leads to the formation of a stabilized polaron pair at the interface before electron transfer proceeds. This intermediate step delays the anion formation to longer time scales, (beyond nanoseconds in the case of DOO-PPV/fullerene blends⁵). Moreover, in certain polymer blend heterojunctions it has been observed that electron transfer can be followed by geminate recombination into an interface exciton or exciplex, inducing a notable reduction of the photovoltaic efficiency.²²

In our system the formation of stabilized polaron pairs after exciton dissociation could be supported by the long-lived dynamics observed at 560 nm with a decay time of 2.4 ns. In addition, the presence of these species could explain the odd increase in photocurrent at low doping levels displayed in Fig. 3. At low concentration of violanthrone, electrons transferred to the dye would remain trapped in small violanthrone domains and the photocurrent would be determined only by holes. On the other hand, the hypothetical formation of polaron pairs in PF_{2/6} prior to electron transfer would enhance the photocurrent due to the likely dissociation experienced by loosely bound polaron pairs under an internal electric field. This process would finally result in an additional contribution of negative carriers to the total photocurrent signal.

IV. CONCLUSION

PLQE measurements in PF_{2/6}/violanthrone blends demonstrate efficient singlet dissociation at the interfaces between

polymer and dye. Photodiodes fabricated from the blends produced a maximum EQE of 3%. This value was achieved in thermally treated devices, where the dye appeared to be arranged in needle-shaped crystals, approximately 250 nm long. In order to better characterize the electron transfer process, pump-probe measurements were carried out on a blend with medium dye content. The experimental results indicate formation of violanthrone anions together with a rise in PF_{2/6} polaron population on a timescale of 7 ps, possibly associated to the average time for the exciton to reach a polymer-dye interface and dissociate. According to this observation, charge transfer is already occurring at early time scales and we have therefore sought to obtain a quantitative picture of the process at 4 ps. At this stage, the increase in PF_{2/6} polaron population suggests that 47% of the total number of excitons have already dissociated into charge pairs. However, only 32% account for the formation of violanthrone anions. We explain these discrepancies between PF_{2/6} polaron and violanthrone anion populations as due to the interplay of stabilized polaron pairs or even exciplexes in the photoinduced electron transfer process.

ACKNOWLEDGMENTS

We thank Covion GmbH and Avecia Ltd for providing the PF_{2/6} polymer and violanthrone dye respectively. J.C.-G. acknowledges financial support from Avecia, The Fundacion Pedro Barrie de la Maza (Spain) and the *European Community-Access to Research Infrastructure action of the Improving Human Potential Programme*, Grant No. HPRI-CT-2001-00148 (Center for Ultrafast Science and Biomedical Optics, CUSBO).

*Email address: juan.cabanillas@polimi.it

- ¹G. Yu, J. Gao, J. C. Hummelen, F. Wudl, and A. J. Heeger, *Science* **270**, 1789 (1995).
- ²N. S. Sariciftci, L. Smilowitz, A. J. Heeger, and F. Wudl, *Science* **258**, 1474 (1992).
- ³J. J. M. Halls, A. C. Arias, J. D. MacKenzie, W. Wu, M. Inbasekaran, E. P. Woo, and R. H. Friend, *Adv. Mater. (Weinheim, Ger.)* **12**, 498 (2000).
- ⁴A. C. Arias, J. D. MacKenzie, R. Stevenson, J. J. M. Halls, M. Inbasekaran, E. P. Woo, D. Richards, and R. H. Friend, *Macromolecules* **34**, 6005 (2001).
- ⁵S. V. Frolov, P. A. Lane, M. Ozaki, K. Yoshino, and Z. V. Vardeny, *Chem. Phys. Lett.* **286**, 21 (1998).
- ⁶C. J. Brabec, F. Padinger, N. S. Sariciftci, and J. C. Hummelen, *J. Appl. Phys.* **85**, 6866 (1999).
- ⁷J. J. Dittmer, E. A. Marseglia, and R. H. Friend, *Adv. Mater. (Weinheim, Ger.)* **12**, 1270 (2000).
- ⁸G. Horowitz, F. Kouki, P. Spearman, D. Fichou, C. Nagues, X. Pan, and F. Garnier, *Adv. Mater. (Weinheim, Ger.)* **8**, 242 (1996).
- ⁹A. J. Makinen, A. R. Melnyk, S. Schoemann, R. L. Headrick, and Y. Gao, *Phys. Rev. B* **60**, 14683 (1999).
- ¹⁰M. Redecker, D. D. C. Bradley, M. Inbasekaran, and E. P. Woo, *Appl. Phys. Lett.* **73**, 1565 (1998).
- ¹¹A. J. Cadby, P. A. Lane, H. Mellor, S. J. Martin, M. Grell, C. Giebeler, D. D. C. Bradley, M. Wohlgenannt, C. An, and Z. V. Vardeny, *Phys. Rev. B* **62**, 15 604 (2000).
- ¹²T. Forster, *Ann. Phys.* **2**, 55 (1948).
- ¹³J. Cabanillas-Gonzalez, Ph.D. thesis, Imperial College, 2003.
- ¹⁴A. Haugeneder, M. Neges, C. Kallinger, W. Spirkl, U. Lemmer, J. Feldmann, U. Scherf, E. Harth, A. Gugel, and K. Mullen, *Phys. Rev. B* **59**, 15 346 (1999).
- ¹⁵J. J. Dittmer, R. Lazzaroni, P. Leclere, M. Granström, K. Petrisch, E. A. Marseglia, R. H. Friend, J. L. Bredas, H. Rost, and A. B. Holmes, *Sol. Energy Mater. Sol. Cells* **61**, 53 (2000).
- ¹⁶J. Cabanillas-Gonzalez, J. Nelson, D. D. C. Bradley, M. Ariu, D. G. Lidzey, and S. Yeates, *Synth. Met.* **137**, 1471 (2003).
- ¹⁷G. Cerullo, S. Stagira, M. Zavelani-Rossi, S. De Silvestri, T. Virgili, D. G. Lidzey, and D. D. C. Bradley, *Chem. Phys. Lett.* **335**, 27 (2001).
- ¹⁸D. W. McBranch, B. Kraabel, S. Xu, R. S. Kohlman, V. I. Klimov, D. D. C. Bradley, B. R. Hsieh, and M. Rubner, *Synth. Met.* **101**, 291 (1999).
- ¹⁹C. Gadermaier, G. Cerullo, G. Sansone, G. Leising, U. Scherf, and G. Lanzani, *Phys. Rev. Lett.* **89**, 117402 (2002).
- ²⁰T. Virgili, D. Marinotto, D. D. C. Bradley, and G. Lanzani, *Appl. Phys. Lett.* (to be published).
- ²¹C. Silva, A. S. Dhoot, D. M. Russell, M. A. Stevens, A. C. Arias, J. D. MacKenzie, N. C. Greenham, R. H. Friend, S. Setayesh, and K. Mullen, *Phys. Rev. B* **64**, 125211 (2001).
- ²²A. C. Morteani, A. S. Dhoot, J. S. Kim, C. Silva, N. C. Greenham, C. Murphy, E. Moons, S. Cina, J. H. Burroughes, and R. H. Friend, *Adv. Mater. (Weinheim, Ger.)* **15**, 1708 (2003).
- ²³P. Vaveliuk, A. M. de Brito Silva, and P. C. de Oliveira, *Phys. Rev. A* **68**, 013805 (2003).
- ²⁴D. R. Waring and G. Hallas, *The Chemistry and Application Of Dyes* (Plenum, New York 1990).